

ORIGINAL ARTICLE

Marta Ferraroni · Wojciech R. Rypniewski
Bruno Bruni · Pierluigi Orioli · Stefano Mangani

Crystallographic determination of reduced bovine superoxide dismutase at pH 5.0 and of anion binding to its active site

Received: 22 December 1997 / Accepted: 30 April 1998

Abstract The crystal structures of dithionite-reduced bovine Cu(I),Zn superoxide dismutase and of its adducts with the inorganic anions azide and thiocyanide have been determined in a $C222_1$ crystal form obtained at pH 5.0. This crystal form is characterized by a high solvent content (72%) and by having the two Cu,ZnSOD monomers (A and B) in different crystal environments. One of them (B) is involved in few intermolecular crystal contacts so that it is in a more “solution like” environment, as indicated by average temperature factors which are about twice those of the other monomer. The differences in crystal packing affect the active site structures. While in the A monomer the Cu(I) is coordinated to all four histidine residues, in the B monomer the bridging His61 side chain is found disordered, implying partial detachment from copper. The same effect occurs in the structures of the anion complexes. The inorganic anions are found bound in the active site cavity, weakly interacting with copper at distances ranging from 2.5 to 2.8 Å. The copper site in the A subunit of the native enzyme structure displays significant electron density resembling a diatomic molecule, bound side-on at about 2.8 Å from the metal, which cannot be unambiguously interpreted. The crystallographic data suggest that the existence of the His61 bridge between copper and zinc is dominated by steric more than electronic factors and that the solution state favors the His61 detachment. These structures confirm the existence of an energetically available state for

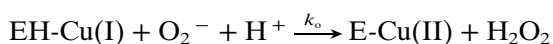
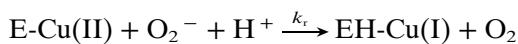
Cu(I) in Cu,ZnSOD where the histidinato bridge to zinc is maintained. This state appears to be favored by tighter crystal contacts. The binding of the anions in the active site cavity is different from that observed in the oxidized enzyme and it appears to be dominated by electrostatic interactions within the cavity. The anion binding mode observed may model the substrate interaction with the reduced enzyme during catalysis.

Key words Reduced Cu,Zn superoxide dismutase · Anion binding · Protein crystallography · Crystal packing effects · Mechanism

Introduction

Cu,Zn superoxide dismutase (Cu,ZnSOD; E.C. 1.15.1.1) is an enzyme ubiquitous in living organisms where it catalyzes the disproportionation of the superoxide radical to dioxygen and hydrogen peroxide, thus protecting the cells from the toxic effects of the O_2^- radical anion [1–3]. The recent demonstration of the involvement of Cu,ZnSOD point mutants in FALS syndrome [4–6] has refueled the interest in the enzyme and its function.

The enzyme from bovine erythrocytes is a homodimer of molecular weight approximately 32 kDa. Each monomer contains one Cu(II) and one Zn(II) ion in the active site, but only the copper ion is essential for catalysis [2, 3, 7]. Cu,ZnSOD is characterized by very high catalytic rates which are diffusion controlled [8, 9]. It is generally accepted that the reaction mechanism proceeds in two steps [9, 10] with approximately equal rate constants for the two reactions ($k_r = k_o \approx 2-3 \times 10^9 \text{ M}^{-1} \text{ s}^{-1}$) [10–12]:



During the catalytic cycle the copper ion alternates between the +2 and +1 oxidation states, as indicated by

S. Mangani (✉)

Department of Chemistry, University of Siena,
Pian dei Mantellini 44, I-53100 Siena, Italy
e-mail: mangani@unisi.it, Fax: +39-577-280405

M. Ferraroni · B. Bruni · P. Orioli
Department of Chemistry, University of Florence,
Via Gino Capponi 7, I-50100 Florence, Italy

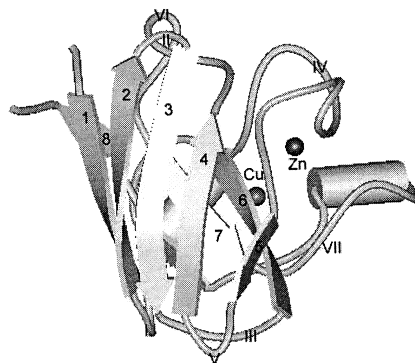
M. Ferraroni · W.R. Rypniewski
EMBL Outstation, c/o DESY, Notkestrasse 85,
D-22603 Hamburg, Germany

the bleaching of the enzyme green-blue color at steady state [13, 14]. The oxidized enzyme has been well characterized by X-ray studies and by several chemical and physical methods [3] (and references therein). The crystal structures of Cu,ZnSOD from bovine, human, and amphibian erythrocytes have been reported, as well as Cu,ZnSOD from yeast, spinach, and a prokaryote [15–20]. All the above structural determinations show that each Cu,ZnSOD monomer maintains the characteristic tertiary structure consisting of a flattened, anti-parallel β -barrel of eight strands joined by seven turns and loops (numbered I to VII following Getzoff et al. 1989 [21]). The active site is located in-between the external wall of the β -barrel and the extended loop VII at the bottom of a conical narrow cavity shaped to accommodate the superoxide substrate. The cavity is surrounded by charged residues which are supposed to provide electrostatic guidance to the substrate [22, 23]. The cavity hosts one copper and one zinc ion. The copper ion is coordinated by the nitrogen atoms of four histidines and by a loosely bound water molecule. One of the histidines (His61 in the bovine SOD sequence) normally bridges copper and zinc. The coordination of zinc is completed by two other histidines and an aspartate group in a tetrahedral geometry. Sketches of the Cu,ZnSOD monomer fold and of the active site cavity displaying the secondary structure numbering and the relevant active site residues, respectively, are shown in Schemes 1 and 2.

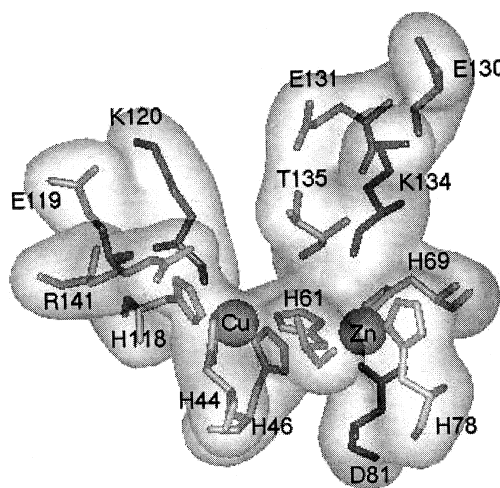
Owing to the inaccessibility of Cu(I) to EPR and electronic spectroscopy, a lesser amount of data is available on the reduced form of the enzyme. UV/vis spectroscopy on the cobalt derivative both in solution and in the solid state [24, 25], EXAFS data [26], and NMR spectroscopy [27–29] on the Cu(I) containing enzyme have provided evidence for the presence of a tri-coordinate cuprous ion resulting from the breaking of the copper-nitrogen bond of the bridging His61 and simultaneous protonation of its N ϵ 2 atom as required by the mechanism proposed by Tainer et al. [37]. A similar arrangement of the copper coordination has been recently observed in the crystal structure of the reduced yeast enzyme from *Saccharomyces cerevisiae* [30]. An EXAFS study, which appeared as the present paper was under preparation, has repeated the measurements published 13 years before [26] and has confirmed the Cu(I) tri-coordination in the bovine Cu(I),ZnSOD solution [31].

In view of the extremely fast rate of the enzyme catalyzed reactions and of experimental evidence such as the equivalence of rate constants for the enzyme in both oxidation states, which point toward small energy differences between the oxidized and reduced enzyme, several authors have proposed different reaction mechanisms implying outer sphere electron transfer without His61 protonation and the consequent breaking of the Cu-His61 bond [32–34].

We have recently determined the crystal structure of the reduced bovine enzyme crystallized in space group



Scheme 1



Scheme 2

$P2_12_12_1$. Our X-ray investigations on a $P2_12_12_1$ crystal form grown at pH 7.5 [35, 36] revealed that, contrary to spectroscopic and to the recent X-ray data, no major structural changes take place upon reduction of the enzyme. In other words, the cuprous ion still appeared to be bound to His61 in bovine Cu(I),Zn SOD.

These new crystallographic findings about the reduced form of Cu,ZnSOD may have mechanistic implications because they imply that, at least under certain circumstances, the enzyme is able to maintain the histidinato bridge between Cu(I) and zinc. It is possible that the crystal structure does not show an active state of the enzyme; nevertheless, the possibility for Cu,ZnSOD to function in this form may settle the debate about how the high catalytic rate of the enzyme can be consistent with a proposed mechanism [37] involving large, energy demanding, active site rearrangements such as the breaking and reforming of the His61 bridge between Cu and Zn and concomitant protonation and deprotonation of the His61 N ϵ 2. At low substrate concentrations, and consequently lower turnover numbers, the enzyme can work with a mechanism involving the breaking of the imidazolate bridge, whereas

under substrate saturating conditions a mechanism with a bridging histidine in both oxidation states would be more satisfying [35].

In addition, since the enzyme shows identical efficiency toward superoxide dismutation in both its oxidized and reduced forms [10–12], it remains a problem to understand the interaction between Cu(I) and the substrate, which in principle should be different from that of Cu(II) in the presence of the imidazolate bridge. For this reason we have decided to determine the crystal structure of complexes of Cu(I),Zn SOD with small mononegative anions such as the isoelectronic azide and thiocyanate, which are inhibitors of the enzyme and have charge and electronic structure similar to the substrate. Hence they should bind to the enzyme in a way resembling that of the superoxide anion and provide clues about its binding to Cu,ZnSOD. Our results will be discussed and compared with those of the recently reported crystal structures of the complexes of oxidized Cu(II),Zn SOD with azide and cyanide anions [38, 39] and with the solution studies on the same complexes [40–42].

Materials and methods

Crystallization

The bovine Cu(I),ZnSOD crystallization solution was prepared from commercially available (Sigma) oxidized enzyme used without further purification. A 7 mg/ml solution of the enzyme at pH 5.0 in 20 mM HEPES buffer was reduced with sodium dithionite under nitrogen atmosphere. Crystals of the adducts Cu(I),ZnSOD-N₃⁻ and Cu(I),Zn SOD-SCN⁻ were obtained by co-crystallization from solutions of the enzyme containing 50 mM and 100 mM inhibitors, respectively. Very large colorless crystals of the native enzyme and of the adducts up to 1.5 × 0.8 × 0.6 mm in size grew in 2 weeks at 22 °C by free interface diffusion in the enzyme solution of a precipitant solution consisting of 20% PEG6000 in the same buffer containing 50 mM and 100 mM NaN₃ or NaSCN in the case of the complexes. All the crystals belong to the orthorhombic space group C222₁ with cell constants: $a=104.6$, $b=197.5$, $c=50.8$ Å with one SOD dimer per asymmetric unit. This new crystal form of Cu,ZnSOD is characterized by the unusually high Matthews parameter of 4.5 Å³/Da [43], which corresponds to a water content of 73%. The oxidation state of the copper ion was checked in every case by single crystal EPR spectroscopy. Figure 1 shows as an example, the EPR spectrum obtained from the Cu(I),ZnSOD-N₃²⁻ crystal used for data collection.

Crystallographic data collection and processing

Three data sets were collected, each from a native reduced crystal (SOD5RN), a thiocyanide soaked reduced crystal (SOD5RSCN), and one from a sodium azide soaked reduced crystal (SOD5RAZ). All data were collected on the EMBL X11 beam line at the DORIS storage ring, DESY, Hamburg, with a 18 cm MarResearch imaging plate scanner. The integrated intensities were measured using the program DENZO and scaled using program SCALEPACK [44]. Relative temperature factors for images were refined. Adjacent partially recorded reflections were scanned. Outliers were rejected based on the χ^2 test implemented in SCALEPACK. The postrefinement option of SCALEPACK was used to refine the cell parameters. Crystals belong to space group

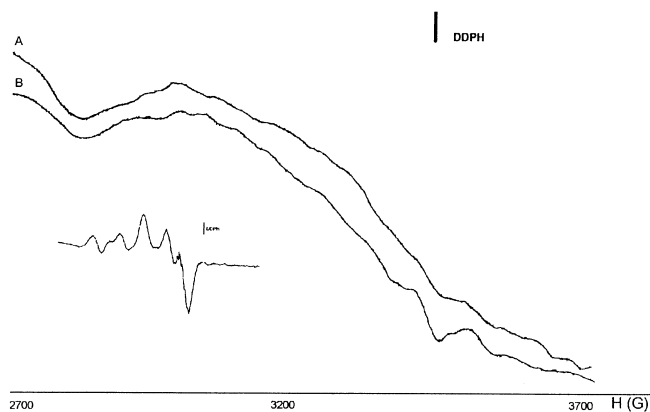


Fig. 1 **A** The spectrum of the Cu(I),ZnSOD crystal used for data collection (**A**) compared with the EPR signal from the empty capillary tube used for the experiment (**B**). The line drift is due to the high gain used. For comparison the EPR spectrum of a Cu(II),ZnSOD crystal is shown in the *inset*

C222₁, with $a=104.6$ Å, $b=197.5$ Å, $c=50.8$ Å. There were no significant differences in the cell parameters between the three data sets. The crystal data and statistics are summarized in Table 1. The intensities were converted to structure factor amplitudes and a correction was applied to weak or negative measurements based on the a priori distribution [45].

Structure solution

The SOD5RN structure was determined by the method of molecular replacement implemented in the program AMORE [46] from the CCP4 program suite [47]. The rotation function was calculated using terms between 10.0 and 3.0 Å, with the Patterson search radius of 20.0 Å. A solution was obtained using, as the starting model, the B subunit of the $P2_12_12_1$ structure of reduced SOD [36]. The two highest peaks in the rotation function had correlation coefficients of 0.32 and 0.20, with other peaks forming a plateau at a correlation coefficient of approximately 0.1. In the translation function these peaks gave correlation coefficients of 0.55 and 0.32, with the remaining peaks forming a plateau at a correlation coefficient of approximately 0.15. Calculating the translation function for the second highest peak, while including the first solution in fixed position, gave a correlation coefficient of 0.77. Rigid body refinement of positions corresponding to the two highest peaks gave a correlation coefficient of 0.81.

The two model monomers were positioned in the unit cell and found to form a single molecular dimer, with inter-subunit contacts similar to those observed in the $P2_12_12_1$ crystal structure. The structure has an unusually high solvent content, with $V_M=4.5$ Å³/Da, from which the solvent content can be estimated at 73% [43].

Refinement

Refinement of atomic coordinates and temperature factors was carried out by stereochemically restrained least-squares minimization [48, 49] as implemented in program PROLSQ from the CCP4 program suite. No σ cut-off was applied to amplitudes. The initial model for the three structures has been the SOD5RN molecular replacement solution. Data between 10.0 Å and the resolution limit were used for refinement in each case. Individual temperature factors were refined in all cycles. The weighting parameters for the refinement and the final values are listed in Table 2. The coordination distances for the metal ions were refined unrestrained. Manual rebuilding of the model was based on ($3F_o-2F_c$) and (F_o-F_c) maps, using an Evans and Sutherland ESV or a Sili-

Table 1 Summary of data

	SOD5RN	SOD5RSCN	SOD5RAZ
Maximum resolution	1.9 Å	2.0 Å	2.05 Å
Wavelength	0.920 Å	0.920 Å	0.920 Å
Number of images	110	131	140
% R_{merge}^*	9.1	7.6	7.4
Raw intensities used	209202	200034	213345
Unique reflections	41816	34111	30955
% Completeness (excl. ∞ -10 Å; highest res. shell in parentheses)	97.2 (98.0)	96.9 (90.7)	87.8 (85.5)
% Greater than 3σ	83.0	80.1	84.3
I/σ in highest res. shell	3.4	3.6	6.6
Postrefined cell parameters (Å):			
<i>a</i>	104.7	104.6	104.6
<i>b</i>	197.8	197.5	197.5
<i>c</i>	50.8	50.8	50.8

* $R_{\text{merge}} = \sum |I_i - \langle I \rangle| / \sum \langle I \rangle$, where I_i is an individual intensity measurement, and $\langle I \rangle$ is the average intensity for this reflection with summation over all the data

Table 2 Refinement data and weighting parameters for the least-squares refinement with the final standard deviations (SD)^a

	SOD5RN		SOD5RAZ		SOD5RSCN		
Atoms refined	2511		2525		2510		
Protein atoms	2127		2164		2142		
Solvent atoms	376		349		356		
Hetero atoms	8		12		12		
Final crystallographic <i>R</i> -factor (all reflections)	0.184		0.166		0.175		
ESD of atomic positions from σ_A plots (Å)	0.15		0.17		0.15		
Refinement weighting:		No. of parameters	SD	No. of parameters	SD	No. of parameters	SD
Bond lengths (Å) (1-2 neighbours)	σ 0.020	2175	0.014	2192	0.018	2190	0.019
Angle distances (Å) (1-3 neighbours)	0.040	2952	0.052	2968	0.028	2965	0.027
Planar distances (Å) (1-4 neighbours)	0.050	710	0.048	710	0.043	710	0.045
Planar groups (Å)	0.020	392	0.011	392	0.018	392	0.018
Chiral volumes (Å ³)	0.150	339	0.146	339	0.182	339	0.179

^a The weights correspond to $1/\sigma^2$

con Graphics Indigo2 graphics stations and the programs FRODO [50] or TOM (FRODO version for SGI workstations). Solvent molecules were inserted and refined using the program ARP [51], with real space positional refinement and automatic determination of statistically significant electron density levels. ARP was set up to remove water molecules from the model if they were found in density less than 0.5σ in the ($3F_o - 2F_c$) map. The threshold level of significant density determined by the program was approximately constant throughout the refinement, close to the 4σ level in the ($F_o - F_c$) map. Potential new water sites had to be within 2.2–3.3 Å of existing atoms in the model. Waters were merged into a single site if the distance between them became less than 2.2 Å. All solvent molecules were refined with occupancy set to 1. Cycles of least-squares refinement were interspersed with rounds of manual rebuilding. The side chains of the residues Lys3, Lys9, Lys23, Gln53, Lys73, Lys89, Ser103 and Lys134 of chain A and of the residues Lys3, Gln15, Lys23, Lys68, Glu75, Lys89, Glu107, Lys120, Arg126, and Lys134 of chain B have been to be found disordered to various extents. In SOD5RN and SOD5RAZ, alternative conformations with fractional occupancy of 0.5 have been found and refined for SerA103 and LysA134, while in SOD5RSCN, C δ was the last visible atom of the LysA134 side chain.

Ramachandran plots [52] for the three structures show that 89.0%, 90.3%, and 89.4% of non-glycine residues lie in the most favored regions of the plot, while 10.6%, 9.2%, and 10.6% fall within the allowed regions for SOD5RN, SOD5RAZ, and

SOD5RSCN, respectively. Only one residue of SOD5RN falls in the so-called generously allowed regions of the plot as defined in the program PROCHECK [53].

Atomic coordinates of the structures have been deposited with the Protein Data Bank [54] with accession codes 1SXN, 1SXZ, and 1XSX.

Results

The overall C222₁ structure

The Cu₂ZnSOD C222₁ crystal form obtained at pH 5.0 is characterized by high solvent content and by an unusually loose packing of the molecules in the cell. The analysis of crystal contacts shows that reduced Cu₂ZnSOD (SOD5RN) makes only 74 intermolecular contacts between 2.4 and 3.7 Å, with symmetry related molecules; 48 of these are subunit A-subunit A interactions involving 10 residues with an average distance of 3.5 Å. Subunit B has only 26 contacts involving six residues, the shortest distance being 3.0 Å with an average of 3.4 Å. This means that the A and B subunits have

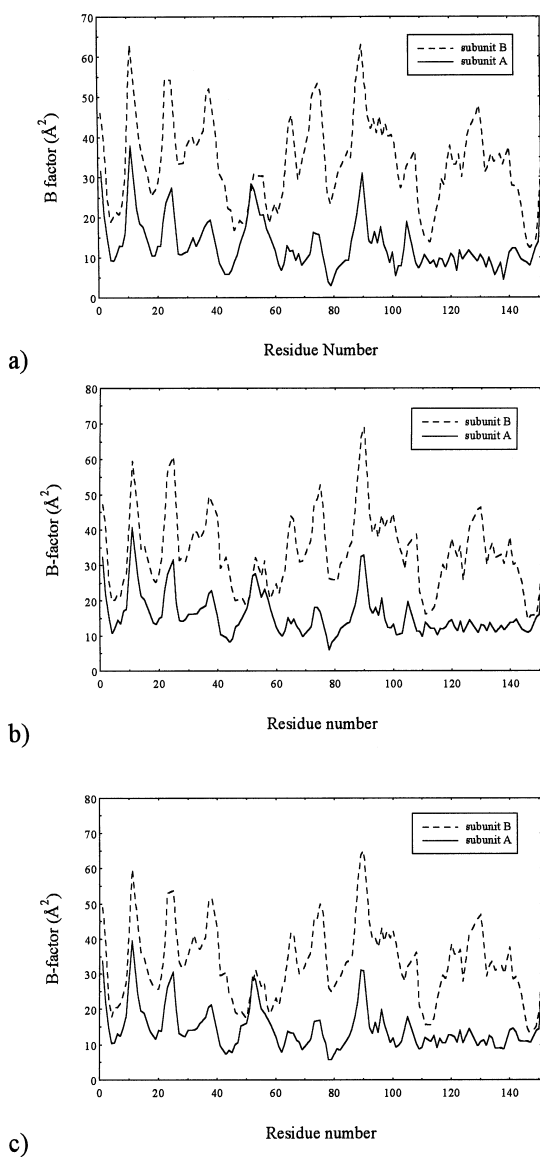


Fig. 2 Main chain temperature factors, averaged for each residue, as a function of residue number, for **a** reduced Cu,ZnSOD at pH=5.0, **b** complex with the azide anion, and **c** complex with the thiocyanate anion

quite different environments in this crystal form, the B subunit being almost completely surrounded by liquid solvent. In other words, the B subunit has a solution-like environment. The above finding is evidenced by the systematically higher temperature factors obtained

Table 3 Average overall temperature factors (\AA^2) for A and B subunits in the three crystal structures

	Subunit A	Subunit B
SOD5RN	14.98	35.15
SOD5RAZ	18.09	36.11
SOD5RSCN	16.42	35.18

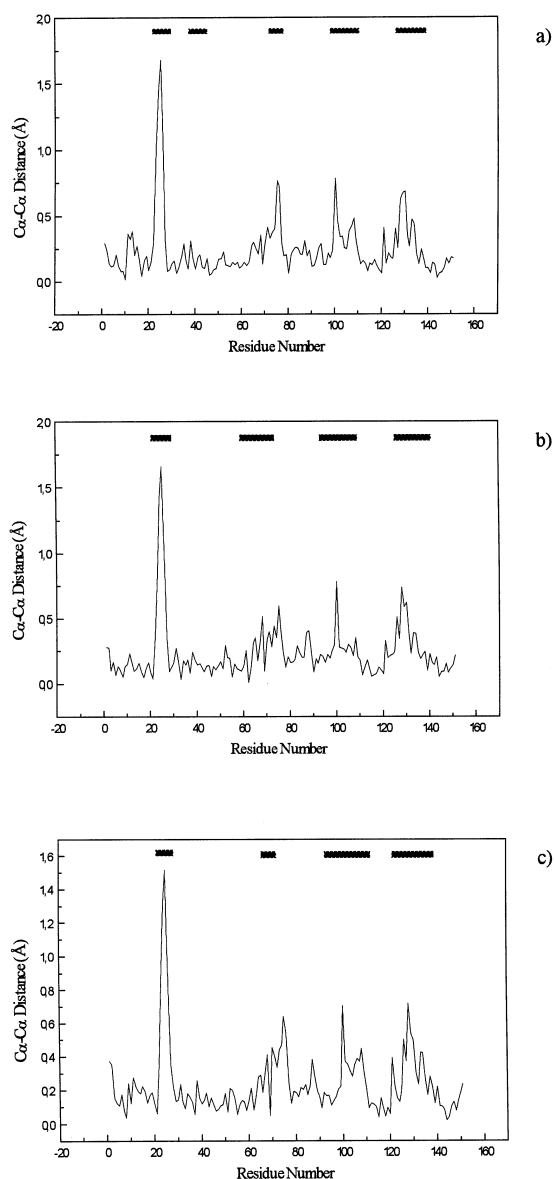


Fig. 3 Differences in coordinates of $C\alpha$ atoms between subunits A and B, superimposed by least-squares minimization for **a** reduced Cu,ZnSOD at pH=5.0, **b** complex with azide anion, and **c** with thiocyanate anion. The *black marks* indicate residue ranges involved in intermolecular contacts. It is evident that these coincide with the zones where the largest $C\alpha$ differences occur

for the B with respect to the A subunit, as shown in Fig. 2 which reports the average main chain atom B-factor per residue for the three crystal structures. Table 3 reports the average temperature factors for each subunit in the three structures; it can be seen that the average temperature factors of the B subunits are double those of the A subunits.

In all three structures, the B subunits appear to be affected by a higher disorder even in the active site. This is apparent from inspection of Fourier difference maps of the A and B sites, where the less resolved electron density of the latter is evident (see Figs. 4–6 be-

low). The unrestrained least-squares refinement of the metal centers always gives higher temperature factors for the metal ions and their ligands in the B with respect to the A sites.

The nature of the difference between A and B subunits is revealed by the plots of the difference between the $C\alpha$ positions in the A and B subunits shown in Fig. 3. Large deviations occur only for Asp25 and for the residues Glu75, Ile102, and Glu130-Ser132. After omitting these residues from the calculations, the overall root mean square displacement (RMSD) between A and B reduces to 0.30, 0.28, and 0.28 Å for the three structures, respectively. This is still about twice the estimated experimental error, meaning that positional differences are significant but small. Thus the main difference between the A and B subunits appears to be the amplitude of the thermal displacements as appreciated by the estimate of $\langle u^2 \rangle (C\alpha \text{ atoms})$ which doubles from about 0.2 to 0.4 Å² in going from A to B.

The overall structure of the Cu,ZnSOD $C222_1$ crystal form obtained at pH 5.0 is conserved with respect to the other structures determined in different space groups. The low pH of the crystallization medium did not influence the enzyme tertiary and quaternary structure. The characteristic Greek-key β -barrel fold of Cu,ZnSOD is present in SOD5RN, SOD5RSCN, and SOD5RAZ with minimal differences with respect to other structural determinations of the reduced and oxidized enzyme at different pH values [15, 30, 38, 39, 55, 56]. Comparison by the least-squares superposition of $C\alpha$ atoms of all the above three structures results in very low deviations (<0.25 Å). However, a close analysis of the structures reveals the presence of small but significant differences, mainly located in the active sites, which deserve a detailed description.

The SOD5RN metal sites

Figure 4a and b shows a stereo view of a $3F_o-2F_c$ Fourier difference map of the metal sites in the A and B subunits of SOD5RN. As already observed in the structure of reduced Cu,Zn bovine SOD at pH 7.5 (1SXC, [36]), in the A subunit the Cu(I) ion appears to be bound to four histidines with the His61 bridge between copper and zinc still in place with a Cu-N ϵ 2(His61) distance of 2.2 Å. On the other hand, His61 in the B subunit appears disordered with its N ϵ 2 at 2.4 Å from copper. However, the most striking feature of the map reporting the site A structure is the occurrence of significant additional electron density in close proximity to the copper ion, which cannot be attributed to the water molecule usually found in the cavity [36]. This density consists of two maxima spaced by 2.1 Å at about 2.7 Å from copper, forming a sort of a hammerhead (see Fig. 4a). However, the electron density map clearly shows the remainder of the metal coordination constituted by the four histidine side chains at distances ranging from 2.1 to 2.3 Å (see Table 4). The above density was evident in the first Fourier maps obtained from the molecular replacement solution of the structure and can be refined either as two oxygen atoms at full occupancy or two sulfur atoms at half occupancy. The refinement as oxygen atoms results in temperature factors of 34.1 and 30.8 Å² while sulfur at half occupancy gives 36.2 and 33.7 Å², respectively. The values of the B-factors obtained, and the shape of the electron density, seem to rule out the presence of mutually exclusive water molecules lying in close sites with partial occupancy. Furthermore, the distance of 2.1 Å between the two peaks excludes the possibility of a dioxygen species in any of its possible oxidation states as well as that of

Fig. 4 Stereoviews of the SOD5RN A(**a**) and B(**b**) copper sites showing a Fourier difference map ($3F_o-2F_c$) contoured at 1.5σ superimposed to the final atomic model. The electron density of the His46 residue has been omitted for clarity

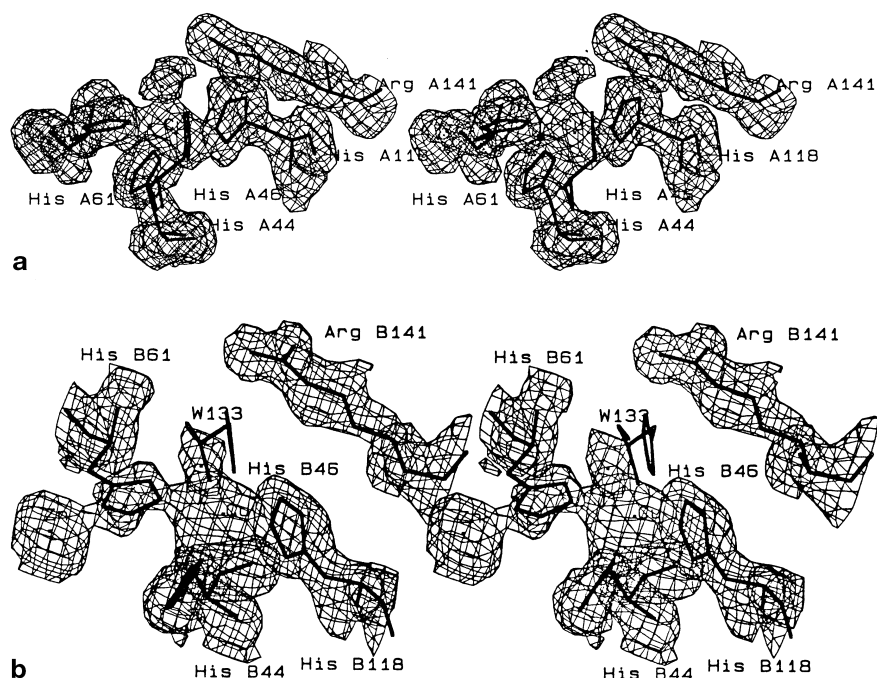


Table 4 Comparison of the bond distances and angles in the Cu(I) and Zn(II) coordination sphere for reduced SOD at pH=5.0 and of the complex with azide and thiocyanate anions.

The distances and angles of reduced SOD at pH 7.5 (SODr) are reported for comparison

	Subunit A				Subunit B			
	SOD5RN	SOD5r-N ₃ ⁻	SOD5r-NCS ⁻	SODr	SOD5RN	SOD5r-N ₃ ⁻	SOD5r-NCS ⁻	SODr
Bond distances (Å)								
Cu-N ^{δ1} His 44	2.1	2.1	2.1	2.2	2.0	1.9	1.9	2.1
Cu-N ^{ε2} His 46	2.3	2.2	2.3	2.2	2.4	2.4	2.4	2.2
Cu-N ^{ε2} His 61	2.2	2.2	2.2	2.3	2.4	2.5	2.3	2.0
Cu-N ^{ε2} His 118	2.1	2.0	2.1	2.2	2.1	2.1	2.1	2.1
Cu-H ₂ O	2.6–2.9 ^a	–	–	~3.0	2.5	–	–	2.1
Cu-N ₃ ⁻	–	2.8	–	–	–	2.5	–	–
Cu-NCS ⁻	–	–	2.8	–	–	–	2.8	–
Zn-N ^{δ1} His 61	2.1	2.0	2.1	2.0	2.1	2.2	2.2	2.1
Zn-N ^{δ1} His 69	2.1	2.1	2.1	2.2	2.3	2.3	2.4	2.2
Zn-N ^{δ1} His 78	1.9	1.9	1.9	2.2	2.0	2.0	2.0	1.9
Zn-O ^{δ1} Asp 81	1.8	1.9	1.8	1.9	1.7	1.8	1.8	2.0

^a The distances for the reduced SOD at pH 7.0 [36] are shown for comparison

two distinct water molecules. On the basis of the distance and in the absence of any other experimental evidence, we may tentatively assign this density to a disulfide anion (S₂²⁻) at partial occupancy, which may have been produced by side reactions (dismutation) of the excess dithionite used for reducing the Cu(II) ion. Statistical analysis of structural data from the Cambridge database indicates an average S-S distance of 2.053(26) Å for the S₂²⁻ anion [57]. The hypothetical disulfide would be oriented side-on with respect to copper.

Evaluation of the copper coordination sphere with the valence sum method [58, 59] results in an oxidation number of 0.91 for a four-coordinated copper in the A subunit. Inclusion of the putative disulfide does not alter the sum because the very long interaction distances with the metal (2.7–2.9 Å) give an oxidation number of 1.00 for six-coordinated copper. Such distances are about 0.5 Å longer than those observed in η² complexes of disulfide with transition metal ions and indicate a merely electrostatic interaction of the putative dianion with the cavity as in the case of the water molecule usually found in this place [16, 37, 55], leaving the Cu(I) cation four-coordinated.

A quite different situation occurs in the B subunit. Here the copper atom appears surrounded by the four histidines, with a water molecule in the fifth position at

2.5 Å. However, as it can be seen in Fig. 4b, the electron density of the water, as well as that of all the other ligands, is more diffuse, indicating disorder. Furthermore, the His61 imidazole ring appears to deviate from the optimal bridging position between copper and zinc. Indeed, in the refined position, the ring plane is such that the Nε2 lone pair is located at about midway between copper and the water molecule which are both at 2.4 Å from Nε2, suggesting the possibility that the modeled ring position is the mean of two unresolved configurations: one corresponding to the usual bridging position and the other to the non-copper bound arrangement due to the breaking of the histidinato bridge between copper and zinc. The His61 disorder is also evidenced by its Nε2 B-factor of 41.4 Å² compared with the average 29.9 Å² of all the four copper-bound histidine-nitrogens from the same subunit. Overall the site appears very disordered with a large spread in ligand distances, which range from the short 2.0 Å of His44 Nε2 to the long 2.4 Å of the His46 Nε2 atom (see Table 4). Even the zinc site in the B subunit seems to be affected by some disorder, as indicated by the wide ligand distance spread and the more distorted geometry with respect to the zinc site in the A subunit (see Table 4).

Inspection of the refined metal ion temperature factors evidences that both A and B copper ions have B-factors significantly higher than those of zinc ions be-

Table 5 Copper ion temperature factors (Å²) compared with the average ligand (L=His44, His 46, His61, His118) temperature factor (Å²). The SD of the average ligand temperature factor is reported in parentheses

	SOD5RN			SOD5RAZ			SOD5RSCN		
	Cu	Zn	L	Cu	Zn	L	Cu	Zn	L
Subunit A	22.4	6.6	8.3 (3.3)	23.8	10.4	11.4 (3.1)	24.1	8.9	10.0 (3.2)
Subunit B	39.6	29.0	25.7 (5.9)	41.2	27.4	27.5 (6.2)	39.9	28.1	26.1 (6.4)

longing to the same subunit and higher than the average temperature factors of the atoms of the histidine ligands, as can be seen from Table 5. The observation is particularly evident for the A subunits and it has also been observed in the other two structures (see Table 5). This result suggests that either the copper sites are characterized by dynamic disorder or that partial release of copper has occurred upon reduction and crystallization. A similar behavior has been observed in the Cu,ZnSOD reduced form at pH 7.5 [36].

Finally, it is interesting to note that the different copper coordination in the A and B subunits can be correlated to the different crystal environment of the two subunits. Indeed, by analyzing the intermolecular contacts made by loops IV and VII, which are the exposed portions of the protein involved in building the active site, we find that the two loops of subunit A make 16 contacts involving 11 different residues while only six contacts involving two residues are present in subunit B, all of them in loop VII.

The SOD5RAZ metal sites

Figure 5a and b reports difference Fourier maps of the copper sites in A and B subunits of SOD5RAZ. Figure 5a clearly shows electron density of elongated shape extending from the copper atom towards the opening of the active site cavity, which can be confidently assigned to a N_3^{2-} anion bound in the site. Refinement with the azide in this density resulted in placing the nearest nitrogen at 2.8 Å from copper with the farthest nitrogen located at contact distances to the side chains of Thr135 and Arg141 (3.4 and 3.5 Å, respectively) and hydrogen-bonded to a water molecule of the cavity (2.3 Å) which is part of a chain of hydrogen-bonded waters extending to the cavity ridge. The Cu(I) ion in the A site is bound

to the four histidines with the His61 Nε2 atom at 2.2 Å and if we take into account the azide molecule as a fifth ligand, its geometry is better described as distorted trigonal bipyramidal where the axial ligands are His61 and His118, the other ligands lying approximately in a plane.

In analogy with the SOD5RN structure, the B subunit presents a different and disordered environment for the metals. Here the four histidines are arranged around copper in a distorted tetrahedral geometry, but electron density interpretable as an azide anion bound to the cavity is found at 2.5 Å from copper. As can be seen from Fig. 5b, this density is not as well defined as that found in the A subunit, indicating partial occupancy and disorder as evident from the azide average temperature factor of 43.4 Å² compared to 33.6 Å² for the azide in subunit A, with the anion nitrogens refined at full occupancy. Also in the B subunit of SOD5RAZ, a large distance spread of the copper and zinc ligands occurs and the refinement places the His61 imidazole ring at 2.5 and 2.3 Å from copper and azide, respectively. Part of the His61 electron density is missing at the 1.5σ level, as evidenced by Fig. 5b, and the Nε2 B-factor is 41.1 Å². The azide-His61 Nε2 distance of 2.3 Å suggests the presence of a strong hydrogen bond which is received by the anion from the detached, protonated Nε2 atom. The azide anion in the B subunit is hydrogen bonded to a water molecule (2.7 Å) and, at variance with the A site, it is within hydrogen bonding distance to a NH₂ group of Arg141 (3.1 Å).

The metal sites in SOD5RSCN

Figure 6a and b reports a difference Fourier map of the A and B copper sites in SOD5RSCN. In both sites, an elongated electron density originating from copper and

Fig. 5 Stereoviews of the SOD5RAZ A (**a**) and B (**b**) copper sites showing a Fourier difference map ($3F_o - 2F_c$) contoured at 1.5σ superimposed to the final atomic model. The electron density of the His46 residue has been omitted for clarity

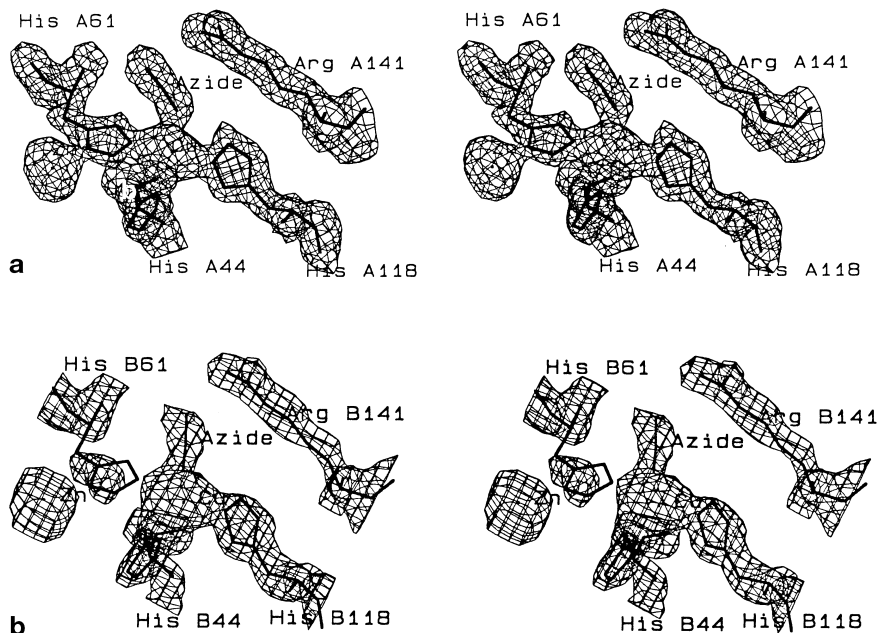
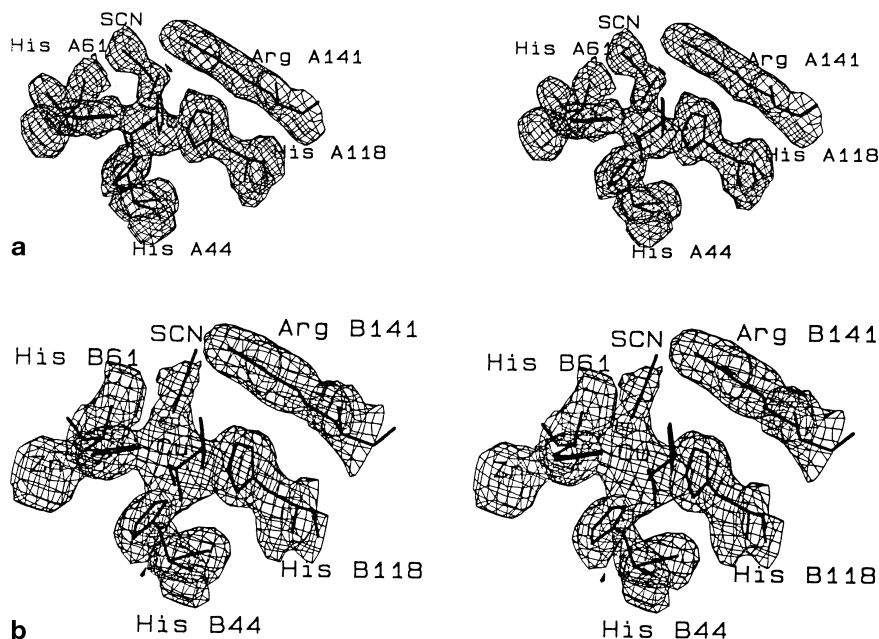


Fig. 6 Stereoviews of the SOD5RSCN A (**a**) and B (**b**) copper sites showing a Fourier difference map ($3F_o - 2F_c$) contoured at 1.5σ superimposed to the final atomic model. The electron density of the His46 residue has been omitted for clarity



extending into the active site cavity is visible, although in the B subunit it is, again, much less intense. The thiocyanate anions were fitted to the densities and refined with the closest atom at about 2.6 \AA from Cu(I) in both the A and B sites. The question arose as to whether the anion approaches copper with the nitrogen or the sulfur atom. In order to gain some insight about this point, the refinement of the closest atom to copper was performed in each case. In both subunits the most realistic temperature factors were obtained with nitrogen (at full occupancy), which refined to 37.6 and 64.8 \AA^2 in A and B, respectively, the temperature factors of the remaining atoms being 45.4 , 44.9 and 70.4 , 80.13 \AA^2 for C and S atoms in the A and B sites respectively. On the other hand, refining the SCN^- copper bound atom as sulfur resulted in unrealistically high temperature factors ($>90 \text{ \AA}^2$). Although this cannot be considered compelling evidence, these results are in favor of a copper-nitrogen interaction with the ligand in the isothiocyanate form. This conclusion is also supported by the visual inspection of the difference electron density maps that, before modeling of the anion, showed the largest and higher electron density in the position far from copper. The unconstrained refinement of the SCN^- anions resulted in a slightly bent molecule with S-C-N angles of 171.9° and 163.1° for the A and B subunits. Angles between 176° and 180° are commonly found in accurate structural determinations of thiocyanate anions [57]. The Cu-N-C (SCN) angles range between 142° and 155° .

The remaining coordination of copper and zinc is quite similar to that already found in both SOD5RN and SOD5RAZ (see Table 4). Once again the copper A site appears more ordered and with a geometry closer to a trigonal bipyramid (His61 and His118 as axial ligands), whereas in the B site it is a distorted tetrahe-

dral structure with a weakly interacting SCN^- . The SCN^- density is weak and at the 1.5σ level is partially missing (Fig. 6b). In subunit A, His61 is bound to Cu(I) at 2.2 \AA while in subunit B this residue is located half way between the SCN^- nitrogen and copper (2.5 and 2.3 \AA , respectively), suggesting again the presence of disorder involving His61 ring motions and detachment from copper. The $N\epsilon 2$ B-factor (40.3 \AA^2) is well above the average B-factor (31.7 \AA^2) of the four copper-bound histidine nitrogens.

Chemical Modification of Glu119

In the present pH 5.0 Cu,ZnSOD reduced form, a chemical modification of the Glu119 side chain is observed in both subunits for all three structures, as already reported for the $P2_12_1$ crystal form of oxidized and reduced Cu,ZnSOD at pH 7.5 [36]. The exact nature of this modification is still unknown. It appears as significant electron density extending from the Glu119 carboxylate group into a maximum at about 2.4 \AA from one of the oxygen atoms. The electron density maximum has been modeled as a calcium ion at 0.5 occupancy.

Discussion

The SOD5RN, SOD5RAZ, and SOD5RSCN structures represent a rare example of a protein crystal where different subunits are subjected to such widely different crystal environments. This has provided the opportunity to observe a direct correlation between crystal contacts and dynamic disorder of the molecule.

The present structures provide an example of how the crystal packing forces may have influence on the protein structure. The 'solution like' environment of the B subunits in these structures results in a sharp increase of the temperature factors for all the atoms with respect to the other subunit. The analysis of thermal motion indicates that the observed differences between subunits can be attributed mainly to an increase of the RMSD of the atoms. This brings us to the conclusion that the scarcity of crystal contacts for one of the subunits results in the increase of the thermal displacements and not in conformational backbone changes. The absence of significant conformational changes in the protein backbone between the A and B subunits is indicative of the intrinsic robustness of the SOD fold, at least for that part of the protein not involved in the monomer-monomer interface. Furthermore, this finding strongly suggests that the dimeric Cu,ZnSODs overall fold observed in crystals is most probably maintained in solution and that it should be closely similar to that of the active enzyme.

We have observed that differences in RMSDs at the level of 0.2–0.3 Å between backbone atoms do not bring about major changes in the enzyme structure. However, displacements of the same magnitude cause significant and probably mechanistically relevant changes when observed in the coordination sphere of the metals in the active site. In the case of the SOD5RN structure, a remarkably different copper environment has been observed in the A and B sites. A relevant, constant feature appearing in all three structures is the disordered His61 ring observed in the B sites. The position of the imidazole ring obtained from the least-squares refinement has not been found in previous bovine Cu,ZnSOD X-ray structures and appears to be a mean between a bridging and a detached position. This is reminiscent of what has been observed in the R32 crystal form of Cu,ZnSOD from yeast (PDB codes 1JCV, 1JCW, 1YSO) [30], where His63 (His61 in the bovine sequence) is found detached at about 3.0 Å from copper. In this case the enzyme was not treated with reducing agents and the finding has been interpreted as a consequence of the spontaneous reduction of the copper center [30]. Interestingly, the R32 crystal form is also characterized by a high solvent content (60–62%; $V_M = 3.1\text{--}3.2 \text{ \AA}^3/\text{Da}$). Our findings bring support to a different hypothesis, namely that the copper reduction is not a sufficient condition for histidine detachment when the protein is in the solid state; a 'solution-like' environment is also needed in order to release the imidazole group from the copper coordination. Indeed, our previous crystal structure determination of reduced Cu,ZnSOD in the $P2_12_12_1$ space group, where the two subunits had similar crystalline contacts, did not reveal any sign of His61 bridge breaking [36]. In other words, our data seem to point out that the stability of the imidazolite bridge between copper and zinc in the crystal appears to be dominated by steric more than electronic factors. Furthermore, it must be stressed that the crys-

tallographic data, compared with the evidence obtained from solution studies, indicate that the two Cu(I),ZnSOD states corresponding to 'bridge broken' and to 'bridge formed' should be energetically very close and separated by small energy barriers. The main point raised by our crystallographic investigations of reduced Cu,ZnSOD is, in our opinion, that the enzyme has both states available. The question about which of them has mechanistic relevance is still open since no experimental evidence has been provided so far about the structure of the working enzyme. It is also possible that the enzyme may work with different mechanisms depending on substrate concentrations, as already pointed out in our previous papers [35, 36].

It must be also pointed out that we have observed His61 disorder, compatible with its detachment from copper, in crystals grown at pH 5.0. This is the low end of the pH range where Cu,ZnSOD is fully active [3] and the pH used in the NMR measurements which provided the only evidence available of a proton bound to His63 (His61 in bovine SOD) in a solution of the human reduced enzyme [27, 29]. The influence of pH on the protonation of the bridging histidine cannot be ruled out. Indeed, studies on model compounds have shown that the binding of a metal ion to a histidine imidazole nitrogen can lower the pK_a of the other NH group by several pH units [60]. The metal ion binding to histidine thus promotes the substitution of the free NH proton by a second metal ion so as to cause an apparent reduction of the pK_{a2} as large as 10 pH units (from 14.4 to about 5.0). It is then possible that at pH 5.0 the proton competes with Cu(I) toward imidazolite binding.

The other relevant point addressed by the SOD5RAZ and SOD5RSCN structures is the interaction of the reduced enzyme with monovalent anions, which may give clues about the part of the enzyme mechanism involving the reoxidation step where Cu(I) is converted back to Cu(II) by a second superoxide molecule.

In every structure we have found the anions bound to the cavity in both subunits, where they are located between copper and the positively charged Arg141. The observed distances between the anions and Cu(I) indicate weak interactions with the metal; however, significant electron density connects in every case the anions with copper (Figs. 5, 6). In SOD5RAZ the Cu-N distances range between 2.5 and 2.8 Å and are significantly larger than the bond distances observed between azide and Cu(II) in the $P2_12_12_1$ form of bovine Cu,ZnSOD, which range between 1.97 and 2.18 Å [38]. This behavior perfectly matches what is expected since both azide and thiocyanide have lesser affinity for four-coordinated Cu(I) due to the reduced positive charge on the metal. Indeed, azide does not have important effects on the copper coordination sphere, contrary to what is observed on the oxidized enzyme, both in solution and in the solid state, where azide displaces Cu(II) from its original position with consequent lengthening

of the Cu-His46 bond [38, 42]. The strong ligand cyanide behaves similarly toward Cu(II), Zn SOD [61].

Even though the difference between the two Cu(I)-azide distances found in A and B subunits is barely significant, it is tempting to speculate that in the B subunit the azide can make a closer approach to Cu(I) when His61 is displaced from its coordination position thanks to a hydrogen bond which may be received from the protonated His61 N ϵ 2 atom (2.3 Å).

The binding modes observed for the competitive inhibitor azide and for the inhibitor thiocyanide may be relevant for the catalytic mechanism of Cu,ZnSOD enzymes. Indeed, if we assume a similar behavior for the superoxide molecule, we may consider the present structures as representative of two possible states along the reaction coordinate. The first is referring to the state where one superoxide molecule has reduced Cu(II) to Cu(I) and lengthens its interaction with the metal just before leaving as a dioxygen molecule. The second refers to the reoxidation step where a superoxide molecule is bound to Cu(I) in order to convert it back to Cu(II). It must be noticed that our observations cannot help in discriminating between the proposed inner and outer sphere mechanisms for Cu,ZnSOD since both predict at least one of the two above states [33, 37]. Finally, the observation of the unexpected electron density close to copper in SOD5RN needs further investigation since, if it really shows a diatomic molecule bound to the site, it would represent a new small molecule binding mode in the Cu,ZnSOD cavity.

Acknowledgements The authors thank the European Union for support of the work at EMBL Hamburg through the HCMP Access to Large Installation Project, Contract Number CHGE-CT93-0040. S.M. also thanks the Italian MURST "Programma di Ricerche di Rilevante Interesse Nazionale" for partially financing this work.

References

- Fridovich I (1986) *Adv Enzymol Relat Areas Mol Biol* 58:61–97
- Bannister JV, Bannister WH, Rotilio G (1987) *CRC Crit Rev Biochem* 22:111–180
- Bertini I, Mangani S, Viezzoli MS (1998) In: Sykes L (ed) *Advances in inorganic chemistry*, vol. 45: Academic Press New York, pp 127–250
- Rosen DR, Siddique T, Patterson D, Figlewicz DA, Sapp P, Hentati A, Donaldson D, Goto J, O'Regan J, Deng H-X, Rahmani Z, Krizus A, McKenna-Yasek D, Cayabyab A, Gattson SM, Berger R, Tanzi RE, Halperin JJ, Herzfeldt B, van der Bergh R, Hung W-Y, Bird T, Deng G, Mulder DW, Smyth C, Laing NG, Soriano E, Pericak-Vance MA, Haines J, Rouleau GA, Gusella JS, Horvitz HR, Brown RH Jr (1993) *Nature* 362:59–62
- Deng H-X, Hentati A, Tainer JA, Iqbal Z, Cayabyab A, Hang W-Y, Getzoff ED, Hu P, Herzfeldt B, Roos RP, Warner C, Deng G, Soriano E, Smyth C, Parge HE, Ahmed A, Roses AD, Hallewell RA, Pericak-Vance MA, Siddique T (1993) *Science* 261:1047–1051
- Wiedau-Pazos M, Goto JJ, Rabizadeh S, Gralla EB, Roe JA, Lee MK, Valentine JS, Bredesen DE (1996) *Science* 271:515–518
- McCord JM, Fridovich I (1969) *J Biol Chem* 244:6049–6055
- Fielden EM, Roberts PB, Bray RC, Lowe DJ, Mautner GN, Rotilio G, Calabrese L (1974) *Biochem J* 139:49–60
- Fee JA, Bull C (1986) *J Biol Chem* 261:13000–13005
- Klug D, Rabani J, Fridovich I (1972) *J Biol Chem* 247:4839–4842
- Rotilio G, Bray RC, Fielden EM (1972) *Biochim Biophys Acta* 268:605–609
- Klug-Roth D, Fridovich I, Rabani J (1973) *J Am Chem Soc* 95:2786–2790
- Klug D, Fridovich I, Rabani J (1973) *J Am Chem Soc* 95:2786–2790
- Fielden EM, Roberts PB, Bray RC, Rotilio G (1973) *Biochem Soc Trans* 1:52–53
- Tainer JA, Getzoff ED, Beem KM, Richardson JS, Richardson DC (1982) *J Mol Biol* 160:181–217
- Parge HE, Hallewell RA, Tainer J (1992) *Proc Natl Acad Sci USA* 89:6109–6114
- Desideri A, Falconi M, Polticelli F, Bolognesi M, Djinovic K, Rotilio G (1992) *J Mol Biol* 223:337–342
- Djinovic K, Gatti G, Coda A, Antolini L, Pelosi G, Desideri A, Falconi M, Marmocchi F, Rotilio G, Bolognesi M (1991) *Acta Crystallogr B* 47:918–927
- Kitagawa Y, Tanaka N, Hata Y, Kusunoki M, Lee G, Katsube Y, Asada K, Alibara S, Morita Y (1991) *J Biochem* 109:447–485
- Bourne Y, Redford SM, Steinmann HM, Lepock JR, Tainer JA, Getzoff ED (1996) *Proc Natl Acad Sci USA* 93:12774–12779
- Getzoff ED, Tainer JA, Stempien MM, Bell GI, Hallewell RA (1989) *Proteins: Struct Funct Genet* 5:322–336
- Getzoff ED, Tainer JA, Weiner PK, Kollman PA, Richardson JS, Richardson DC (1983) *Nature* 306:287–290
- Fisher CL, Cabelli DE, Hallewell RA, Beroza P, Lo TP, Getzoff ED, Tainer JA (1997) *Proteins: Struct Funct Genet* 29:103–112
- McAdam ME, Fielden EM, Lavelle F, Calabrese L, Cocco D, Rotilio G (1977) *Biochem J* 167:271–274
- Merli A, Rossi G, Djinovic K, Bolognesi M, Desideri A, Rotilio G (1995) *Biochem Biophys Res Commun* 210:1040–1044
- Blackburn NJ, Hasnain SS, Binsted N, Diakun GP, Garner CD, Knowles PF (1984) *Biochem J* 219:985–990
- Bertini I, Luchinat C, Monnanni R (1985) *J Am Chem Soc* 107:2178–2179
- Bertini I, Capozzi F, Luchinat C, Piccioli M, Viezzoli MS (1991) *Eur J Biochem* 197:691–697
- Bertini I, Luchinat C, Piccioli M, Vicens Oliver M, Viezzoli MS (1991) *Eur Biophys J* 20:269–279
- Ogihara NL, Parge HE, Hart JP, Weiss MS, Goto JJ, Crane BR, Tsang J, Slater K, Roe JA, Valentine J (1996) *Biochemistry* 35:2316–2321
- Murphy LM, Strange RW, Hasnain SS (1997) *Structure* 5:371–379
- Osman R, Basch H (1984) *J Am Chem Soc* 106:5710–5714
- Osman R (1996) In: Rotilio G (ed) *Superoxide and superoxide dismutase in chemistry, biology and medicine*. Elsevier, New York, pp 141–144
- Rosi M, Sgamellotti A, Tarantelli F, Bertini I, Luchinat C (1986) *Inorg Chem* 25:1005–1008
- Banci L, Bertini I, Bruni B, Carloni P, Luchinat C, Mangani S, Orioli PL, Piccioli M, Rypniewski W, Wilson K (1994) *Biochem Biophys Res Commun* 202:1088–1095
- Rypniewski WR, Mangani S, Bruni B, Orioli PL, Casati M, Wilson KS (1995) *J Mol Biol* 251:282–296
- Tainer JA, Getzoff ED, Richardson JS, Richardson DC (1983) *Nature* 306:284–287
- Djinovic K, Polticelli F, Desideri A, Rotilio G, Wilson K, Bolognesi M (1994) *J Mol Biol* 240:179–183
- Djinovic K, Battistoni A, Carri MT, Polticelli F, Desideri A, Rotilio G, Coda A, Bolognesi M (1994) *FEBS Lett* 349:93–98

40. Bertini I, Luchinat C, Monnanni R, Scozzafava A, Borghi E (1984) *Inorg Chim Acta* 91:109–111
41. Banci L, Bertini I, Luchinat C, Scozzafava A (1989) *J Biol Chem* 264:9742–9744
42. Banci L, Bencini A, Bertini I, Luchinat C, Piccioli M (1990) *Inorg Chem* 29:4867–4873
43. Matthews BW (1968) *J Mol Biol* 33:491–497
44. Otwinowski Z (1993) In: Sawyer L, Isaacs N, Bailey S (eds) *Proceedings of the CCP4 study weekend. data collection and processing*. SERC, Daresbury Laboratory, Chester, pp 56–62
45. French S, Wilson KS (1978) *Acta Crystallogr A* 34:517–525
46. Navaza J (1994) *Acta Crystallogr A* 50:157–163
47. Collaborative Computational Project N4 (1994) *Acta Crystallogr D* 50:760–763 (Abstr)
48. Konnert JH (1976) *Acta Crystallogr A* 32:614–617
49. Konnert JH, Hendrickson WA (1980) *Acta Crystallogr A* 36:344–350
50. Jones TA (1978) *J Appl Crystallogr* 11:268–272
51. Lamzin VS, Wilson KS (1993) *Acta Crystallogr D* 49:129–147
52. Ramachandran GN, Sasisekharan V (1968) *Adv Protein Chem* 23:283–437
53. Laskowski RA, MacArthur MW, Moss DS, Thornton JM (1993) *J Appl Crystallogr* 26:283–291
54. Bernstein FC, Koetzle TF, Williams GJB, Meyer EF Jr, Rodgers JR, Kennard O, Shimanouchi T, Tasumi M (1977) *J Mol Biol* 112:535–542
55. Djinovic K, Gatti G, Coda A, Antolini L, Pelosi G, Desideri A, Falconi M, Marmocchi F, Rotilio G, Bolognesi M (1992) *J Mol Biol* 225:791–809
56. Djinovic K, Coda A, Antolini L, Pelosi G, Desideri A, Falconi M, Rotilio G, Bolognesi M (1992) *J Mol Biol* 226:227–238
57. Orpen G, Brammer L, Allen FH, Kennard O, Watson DG (1989) *J Chem Soc Dalton Trans* S1–S83
58. Thorp HH (1992) *Inorg Chem* 31:1585–1588
59. Liu W, Thorp HH (1993) *Inorg Chem* 32:4102–4105
60. Sundberg RJ, Martin, BR (1974) *Chem Rev* 74:471–517
61. Djinovic Carugo K, Battistoni A, Carri MT, Polticelli F, Desideri A, Rotilio G, Coda A, Bolognesi M (1994) *FEBS Lett* 349:93–98